

 NATIONAL HIGH
MAGNETIC
FIELD LABORATORY

High Field NMR of Quadrupolar Nuclei Using 36 T SCH Magnet

Zhehong Gan

DNP/PANACEA workshop, Tallahassee, Aug 25, 2025



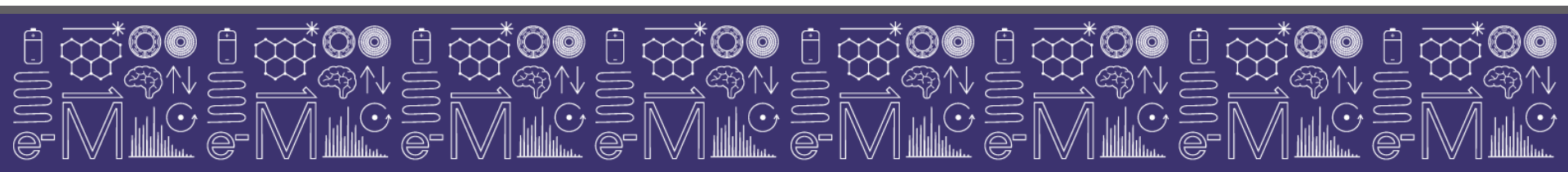
FLORIDA STATE
UNIVERSITY



UF UNIVERSITY of
FLORIDA

Overviews

- **Why we do solid-state NMR of quadrupolar nuclei using SCH**
- **Basics of quadrupolar NMR**
- **Commonly used experiments (MQMAS, QCPMG)**
- **Examples from crystalline to disordered, solids to solution**



NMR of Spin > 1/2 Quadrupolar Nuclei

| | | | | | | | | | | | | | | | | | | | |
|-------------|-------------|-------------|-------------|------------|----------|-------------|--------------|-------------|-----------|-------------|-----------|-------------|-----------|-------------|-----------|-------------|--------------|--|----|
| H 2 | | | | | | | | | | | | | | | | | | | He |
| Li 6,7 | Be 9 | | | | | | | | | B 10,11 | C 12 | N 14 | O 17 | F 19 | Ne 21 | | | | |
| Na 23 | Mg 25 | | | | | | | | | Al 27 | Si 28 | P 31 | S 33 | Cl 35,37 | Ar | | | | |
| K 39,41 | Ca 43 | Sc 45 | Ti 47,49 | V 50,51 | Cr 53 | Mn 55 | Fe 56 | Co 59 | Ni 61 | Cu 63,65 | Zn 67 | Ga 69,71 | Ge 73 | As 75 | Se 78 | Br 79,81 | Kr 83 | | |
| Rb 85,87 | Sr 87 | Y 89 | Zr 91 | Nb 93 | Mo 97 | Tc 99 | Ru 99,101 | Rh 103 | Pd 105 | Ag 107 | Cd 112 | In 113-5 | Sn 117 | Sb 121-3 | Te 127 | I 127 | Xe 129-31 | | |
| Cs 133 | Ba 135-7 | La 138-9 | Hf 177-9 | Ta 181 | W 183 | Re 185-7 | Os 187-9 | Ir 191-3 | Pt 195 | Au 197 | Hg 201 | Tl 203 | Pb 207 | Bi 209 | Po | At | Rn | | |
| Fr | Ra | Ac | | | | | | | | | | | | | | | | | |

| | | | | | | | | | | | | | |
|----|-----------|-------------|----|-------------|-------------|-------------|-----------|-------------|-----------|-----------|----|-----------|-------------|
| Ce | Pr 141 | Nd 143-5 | Pm | Sm 147-9 | Eu 151-3 | Gd 155-7 | Tb 159 | Dy 161-3 | Ho 165 | Er 167 | Tm | Yb 173 | Lu 175-6 |
| Th | Pa | U 235 | Np | Pu | Am | Cm | Bk | Cf | Es | Fm | Md | No | Lr |

- ❖ $I=1/2$ ^1H , ^{19}F , ^{29}Si , ^{31}P ...
- ❖ $I=1$ ^2H , ^6Li , ^{14}N .
- ❖ $I=3/2$ ^7Li , ^{11}B , ^{23}Na , $^{69,71}\text{Ga}$...
- ❖ $I=5/2$ ^{17}O , ^{27}Al ...

- ❖ Low- γ ^{25}Mg , ^{33}S , ^{39}K , ^{43}Ca ,
 $^{45,47}\text{Ti}$, ^{67}Zn , ^{73}Ge , $^{95,97}\text{Mo}$, $^{99,101}\text{Ru}$

- ❖ Glasses, zeolites, catalysts
- ❖ Meso-macro-porous materials
- ❖ Nano materials
- ❖ Battery materials
- ❖ Metal-organic-framework

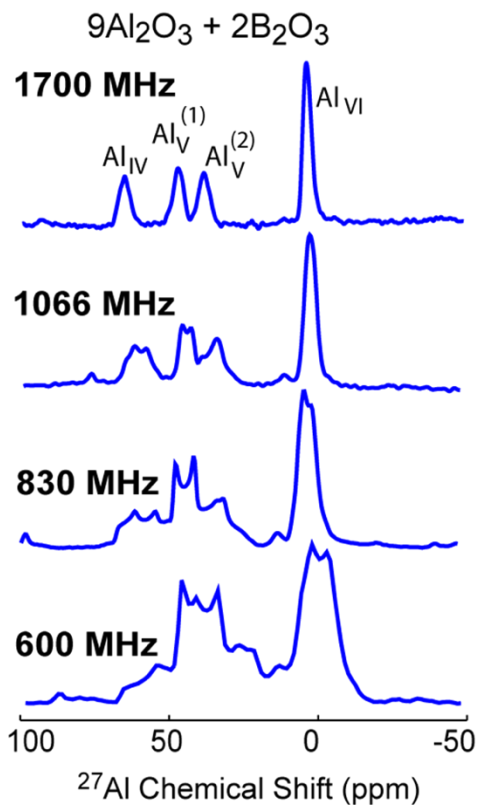
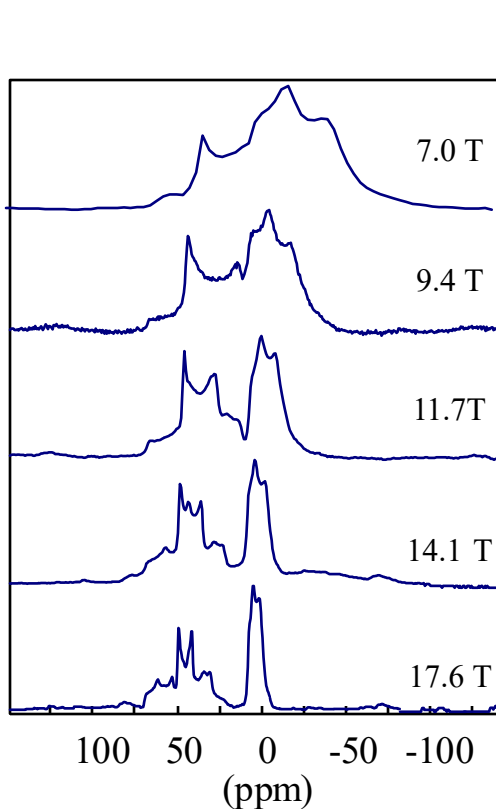
Only $I=1/2$ nuclear spins

Quadrupolar nuclei ($I > 1/2$)

“Solid state NMR measurements in inorganic materials stand to benefit enormously from the availability of high field magnets”. – COHMAG p.36



High Field Quadrupolar Nuclei NMR: Resolution and Sensitivity



NMR signal

Boltzman factor B_0

Frequency B_0

Line narrowing B_0

Resolved spinning sideband

~20 gain in sensitivity

~400 in time

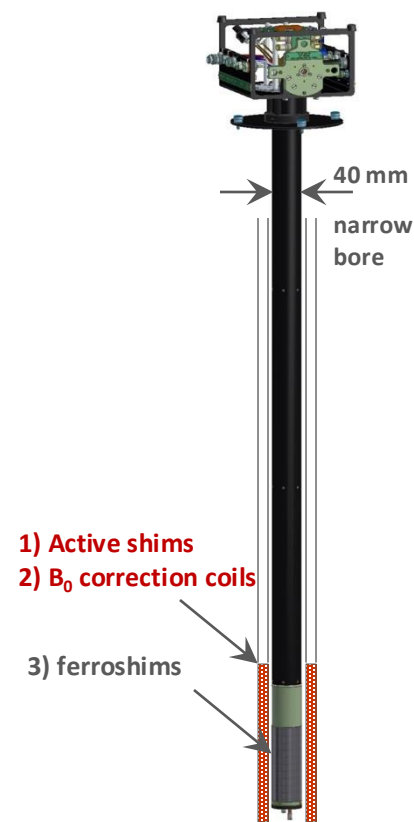
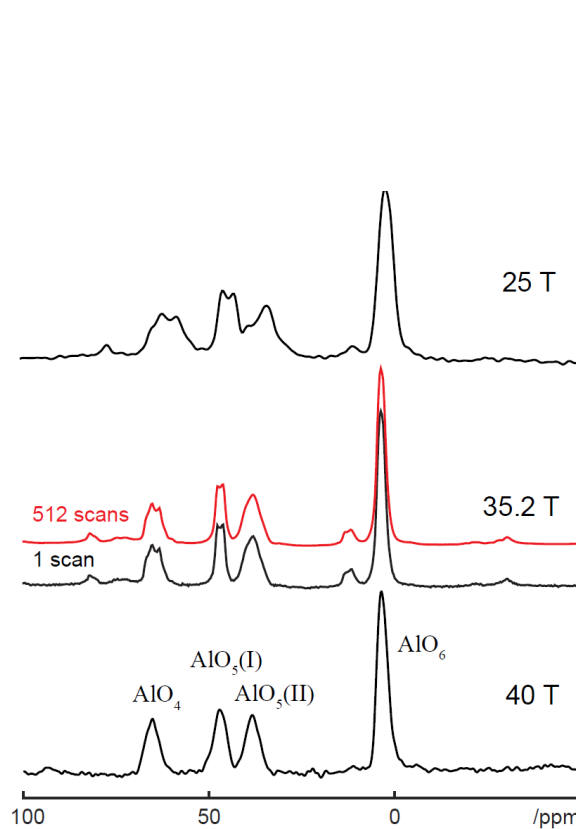
Gan, Z.; Gor'kov, P.; Cross, T. A.; Samoson, A.; Massiot, D. *J. Am. Chem. Soc.* **2002**, *124*, 5634–5635, <https://doi.org/10.1021/ja025849p>

Gan, Z.; Gor'kov, P.; Cross, T. A.; Samoson, A.; Massiot, D. *J. Am. Chem. Soc.* **2002**, *124*, 5634–5635, <https://doi.org/10.1021/ja025849p>

Gan, Z.; Gor'kov, P.; Cross, T. A.; Samoson, A.; Massiot, D. *J. Am. Chem. Soc.* **2002**, *124*, 5634–5635, <https://doi.org/10.1021/ja025849p>

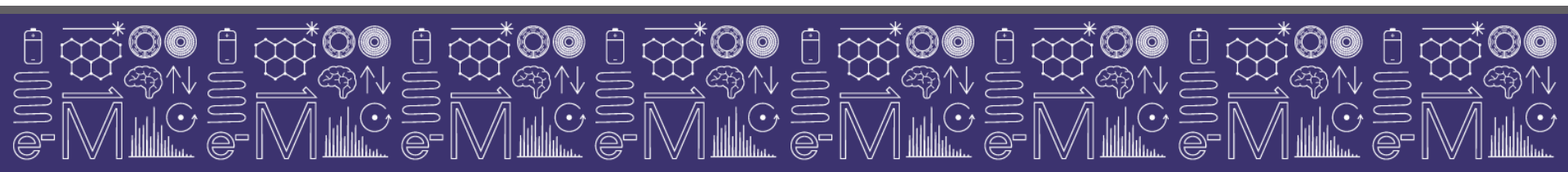
36T Series Connected Hybrid (SCH)

Made to field November 2016, commissioned December 2017

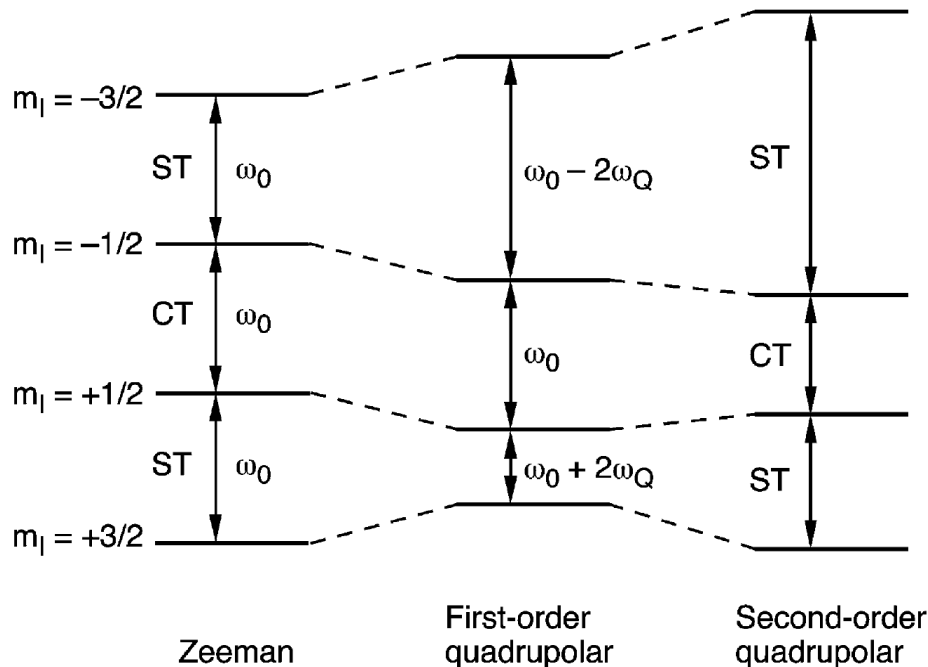


Overviews

- Why we do solid-state NMR of quadrupolar nuclei using SCH
- **Basics of quadrupolar NMR**
- Commonly used experiments (MQMAS, QCPMG)
- Examples from crystalline to disordered, solids to solution



Quadrupolar Nuclei (e.g. spin = 3/2)



- For half-integer Q-nuclei, the central transition (CT) is free of 1st-order effect, broadened only by 2nd-order effect (ω_Q^2/ω_0).
- Satellite transitions (ST) are shifted by large 1st (ω_Q) plus 2nd-order effects.
- 2nd-order effect contains ranks 0, 2, 4 terms, therefore cannot be completely narrowed by magic-angle spinning (MAS).
- For integer Q-nuclei (^{14}N , spin = 1), single-quantum transitions are shifted by 1st and 2nd-order effects.

Quadrupolar broadening and MAS

With sample rotation around β_R

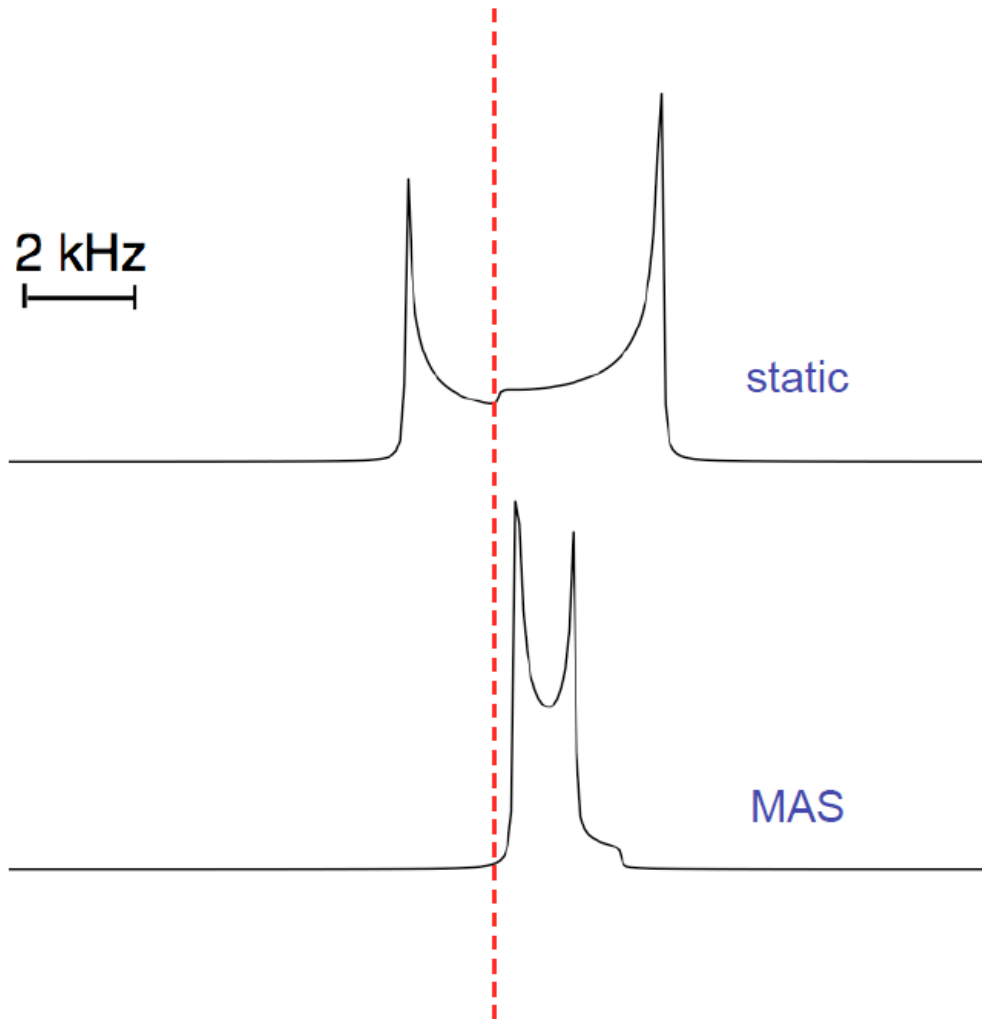
$$\omega \propto \frac{(\omega_Q^{\text{PAS}})^2}{\omega_0} \left[A + B d_{00}^2(\beta_R) d_{00}^2(\beta) + C d_{00}^4(\beta_R) d_{00}^4(\beta) \right]$$

$$d_{00}^2(\beta_R) \propto (3 \cos^2 \beta_R - 1)$$

$$d_{00}^4(\beta_R) \propto (35 \cos^4 \beta_R - 30 \cos^2 \beta_R + 3)$$

- Second-rank term $d_{00}^2(\beta_R) = 0$ when $\beta_R = 54.736^\circ$
- But $d_{00}^4(54.736^\circ) \neq 0$, so although the lineshape is narrowed under MAS the quadrupolar broadening is not completely removed
- To ensure $d_{00}^4(\beta_R) = 0$, β_R must be 30.56° or 70.12°

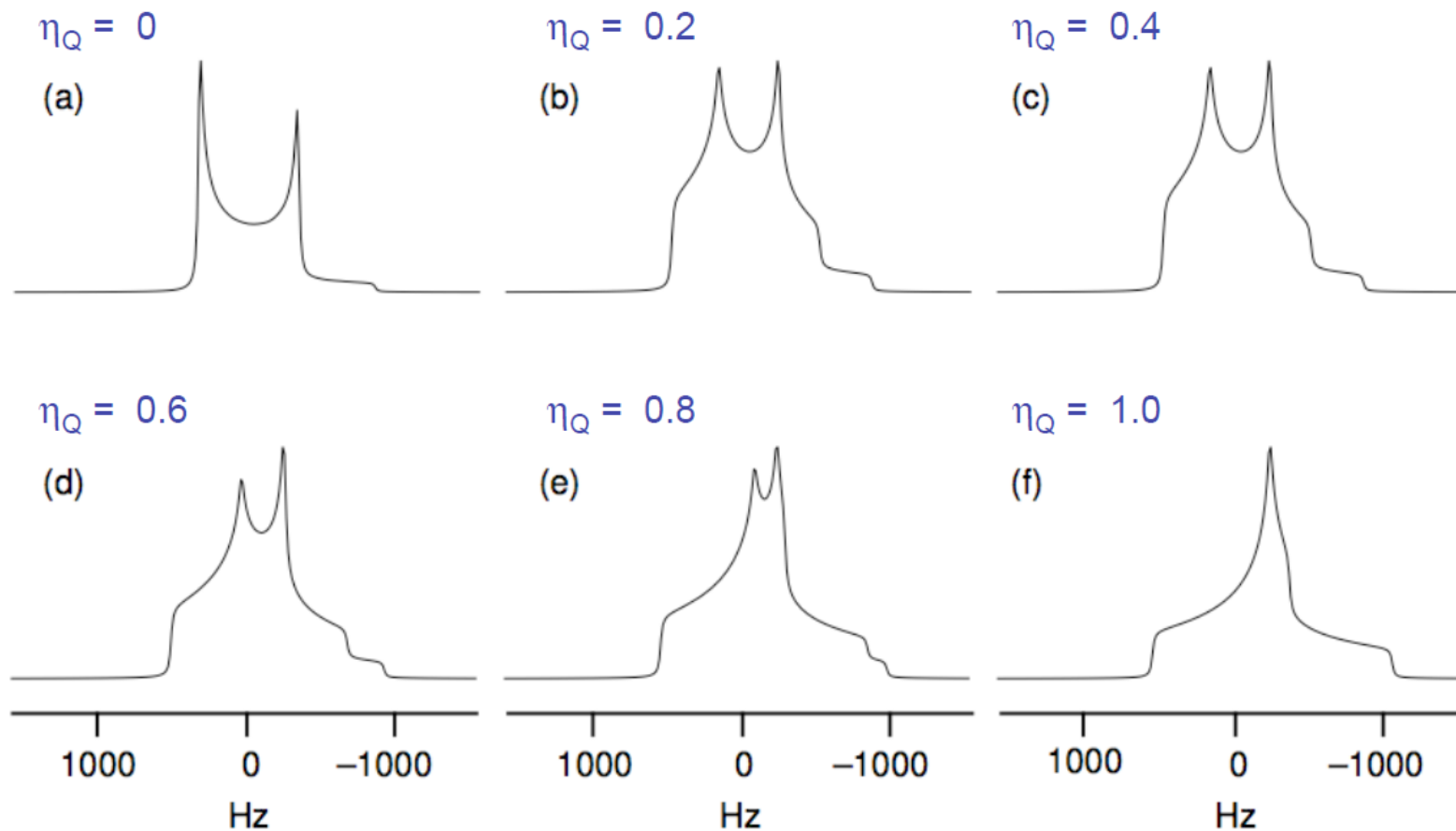
Quadrupolar broadening and MAS



- Lineshape is significantly narrowed by MAS
- Fourth-rank anisotropic quadrupolar broadening remains
- Isotropic quadrupolar shift

$$\propto ((\omega_Q^{PAS})^2/\omega_0) A (1 + \eta_Q^2/3)$$

Spin $I = 3/2$ MAS lineshapes



rf irradiation to a multi-level system

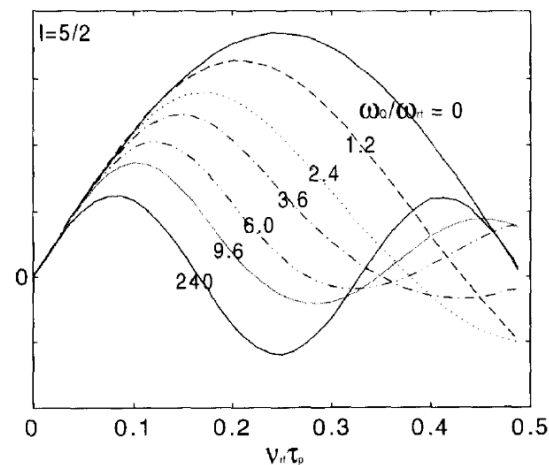
➤ Spin dynamics under *rf* is complicated for the multiple-level systems especially in the presence of level crossing under magic-angle spinning. As the result, spin lock, cross polarization and decoupling become non-trivial and complicated as compared to spin-1/2.

$$\omega_1 \gg \omega_Q^{\text{PAS}}$$

“hard” pulse

“non-selective” pulse

nutration at rate of ω_1



$$\omega_1 \ll \omega_Q^{\text{PAS}}$$

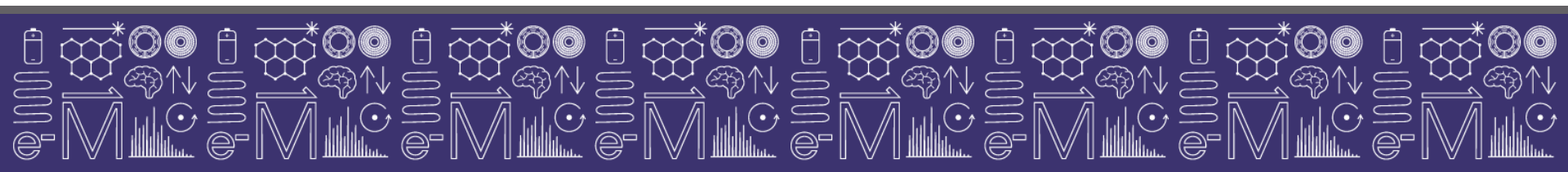
“soft” pulse

“selective” pulse

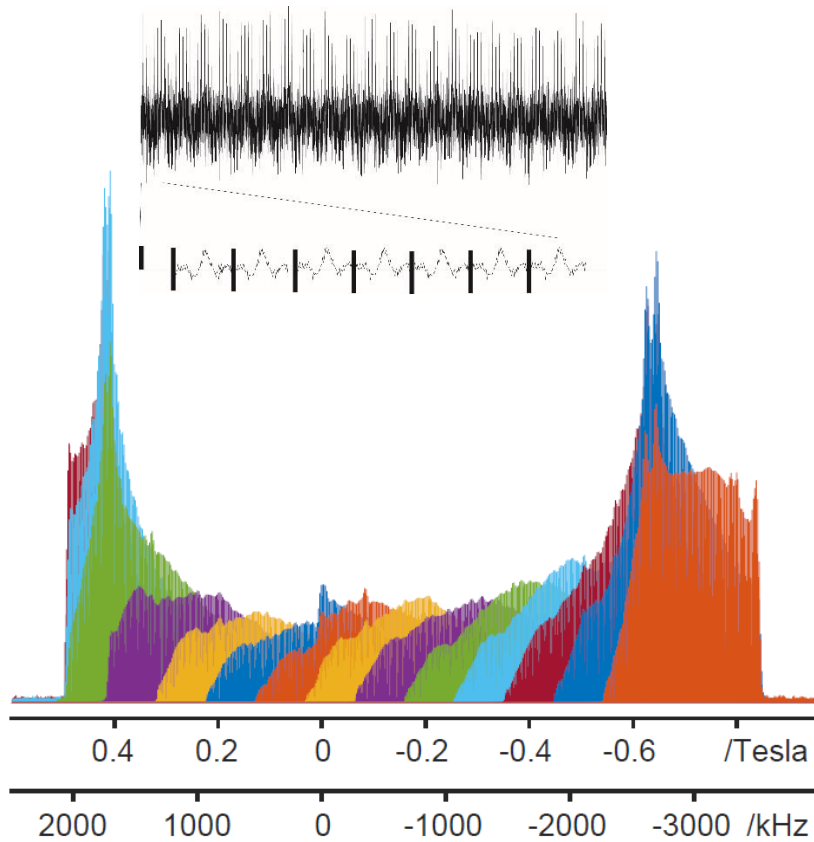
CT nutation rate $(l + 1/2) \omega_1$

Overviews

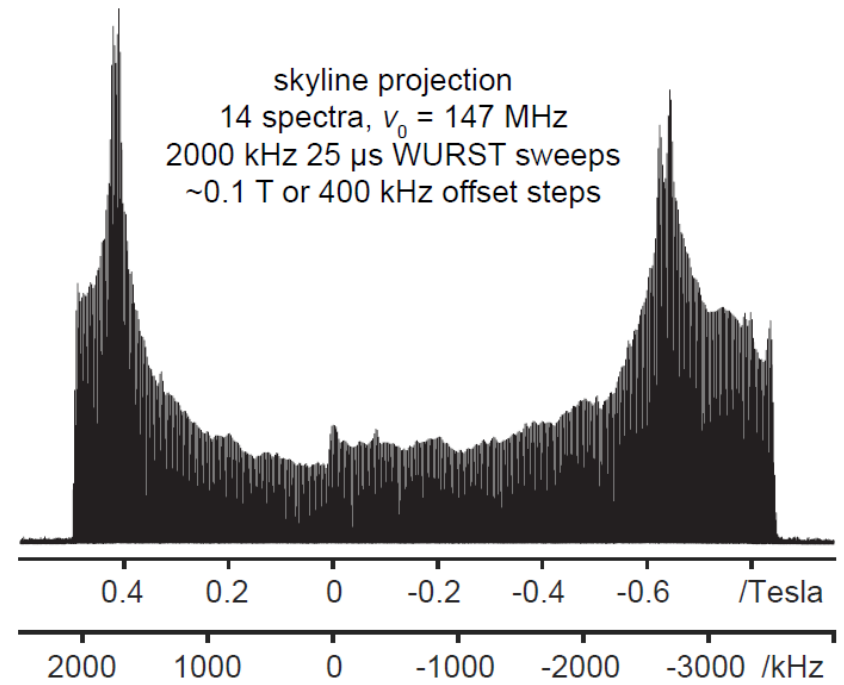
- Why we do solid-state NMR of quadrupolar nuclei using SCH
- Basics of NMR for quadrupolar nuclei
- **Commonly used experiments (MQMAS, QCPMG)**
- **Examples: from crystalline to disordered, solids to solution**



Ultrawide QCPMG by stepping field



^{35}Cl VOCS WURST/CPMG at 35.2 T
of Tetrachloroterephthalonitrile

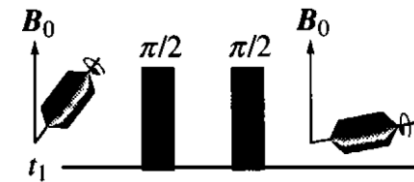


D. Bryce U. Ottawa

Methods to obtain isotropic spectra

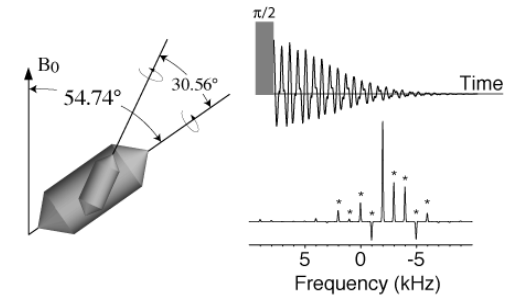
Dynamic Angle Spinning (DAS)

Llor, Virlet (1988), Pines et al (1990)



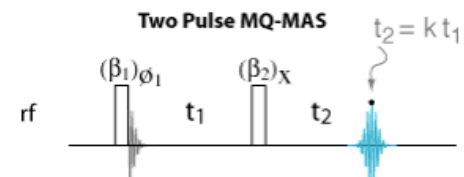
Double Rotation (DOR)

Samoson, Lippmaa, Pines (1990)



Multiple-Quantum MAS (MQMAS)

Frydman and Harwood (1995)



Satellite-Transition MAS (STMAS)

Gan (2000)



Remove Quadrupolar Broadening

$$\omega \propto \frac{(\omega_Q^{\text{PAS}})^2}{\omega_0} \left[A + B d_{00}^2(\beta) + C d_{00}^4(\beta) \right]$$

Constant depending upon C_Q , I and ω_0

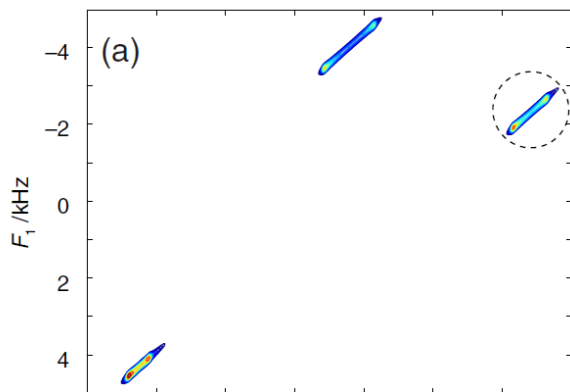
Isotropic shift

Second-rank anisotropic

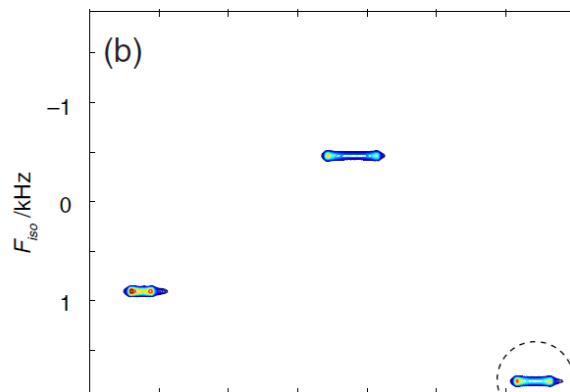
Fourth-rank anisotropic

| Spin | Transition | A | B | C |
|-----------|-----------------|----------|----------|-----------|
| $I = 3/2$ | CT | $-2/5$ | $-8/7$ | $54/35$ |
| | ST | $4/5$ | $4/7$ | $-48/35$ |
| $I = 5/2$ | CT | $-16/15$ | $-64/21$ | $144/35$ |
| | ST ₁ | $2/5$ | $-4/3$ | $6/5$ |
| | ST ₂ | $56/15$ | $80/21$ | $-264/35$ |

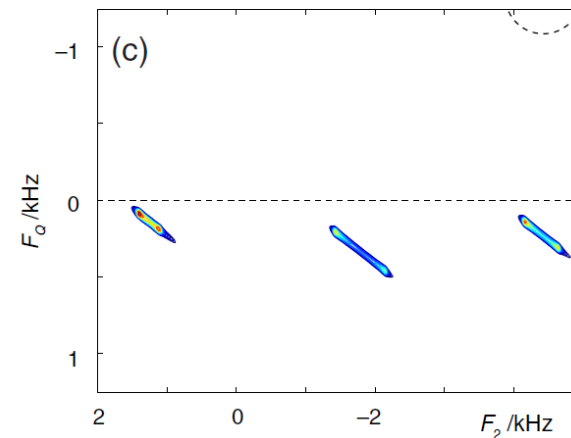
Shearing and representations



Original



Isotropic

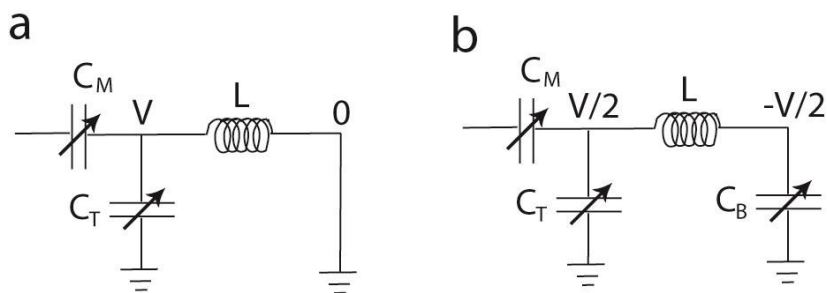


Q-representaion



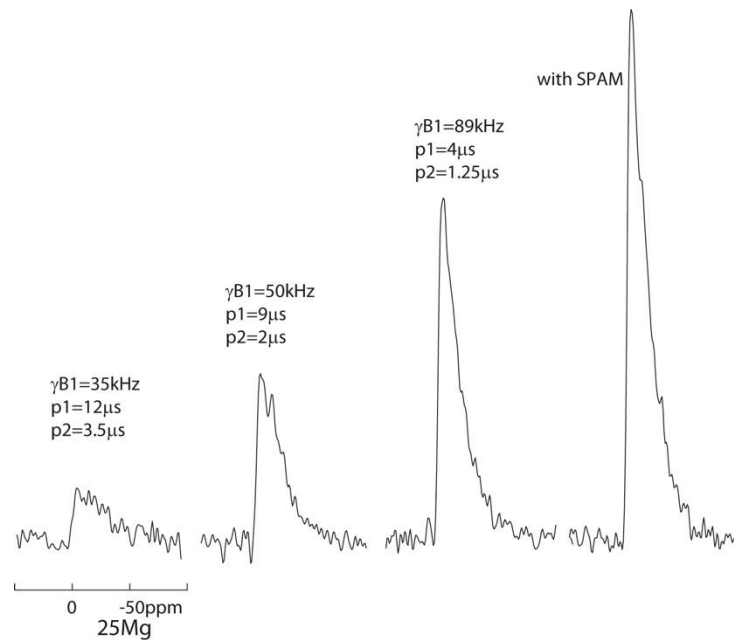
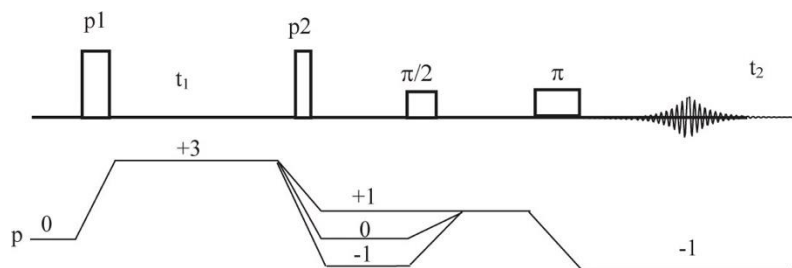
Strong *rf* field

Balanced probe circuit delivers high B_1 field



Sensitivity enhancement with high B_0 , B_1 and SPAM-MQMAS for low- γ nuclei

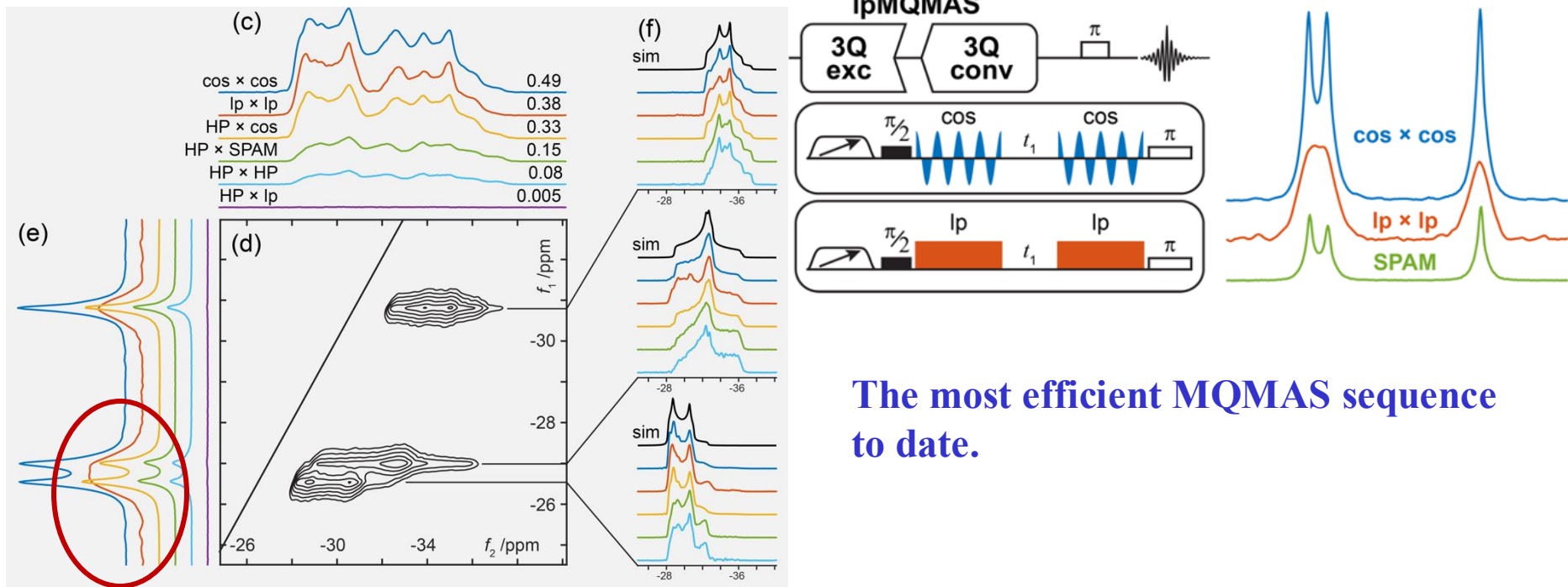
Efficient SPAM-MQMAS pulse sequence



J. Magn. Reson. **200**, (2009) 2-5



Single-frequency vs Double-frequency cosine- I_p MQMAS



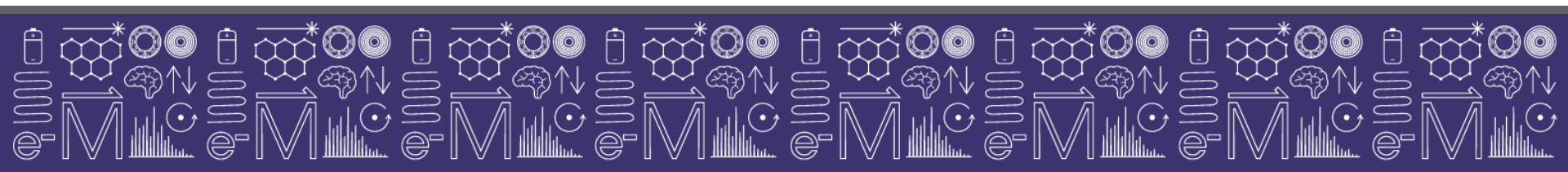
The most efficient MQMAS sequence to date.

Hung, I.; Gan, Z. *J. Magn. Reson.*, 2021,328, 106994 <https://doi.org/10.1016/j.jmr.2021.106994>



Overviews

- Why we do solid-state NMR of quadrupolar nuclei using SCH
- Basics of NMR for quadrupolar nuclei
- Commonly used experiments (MQMAS, QCPMG)
- **Examples: from crystalline to disordered, solids to solution**



^{39}K MQMAS

from small to macro molecules

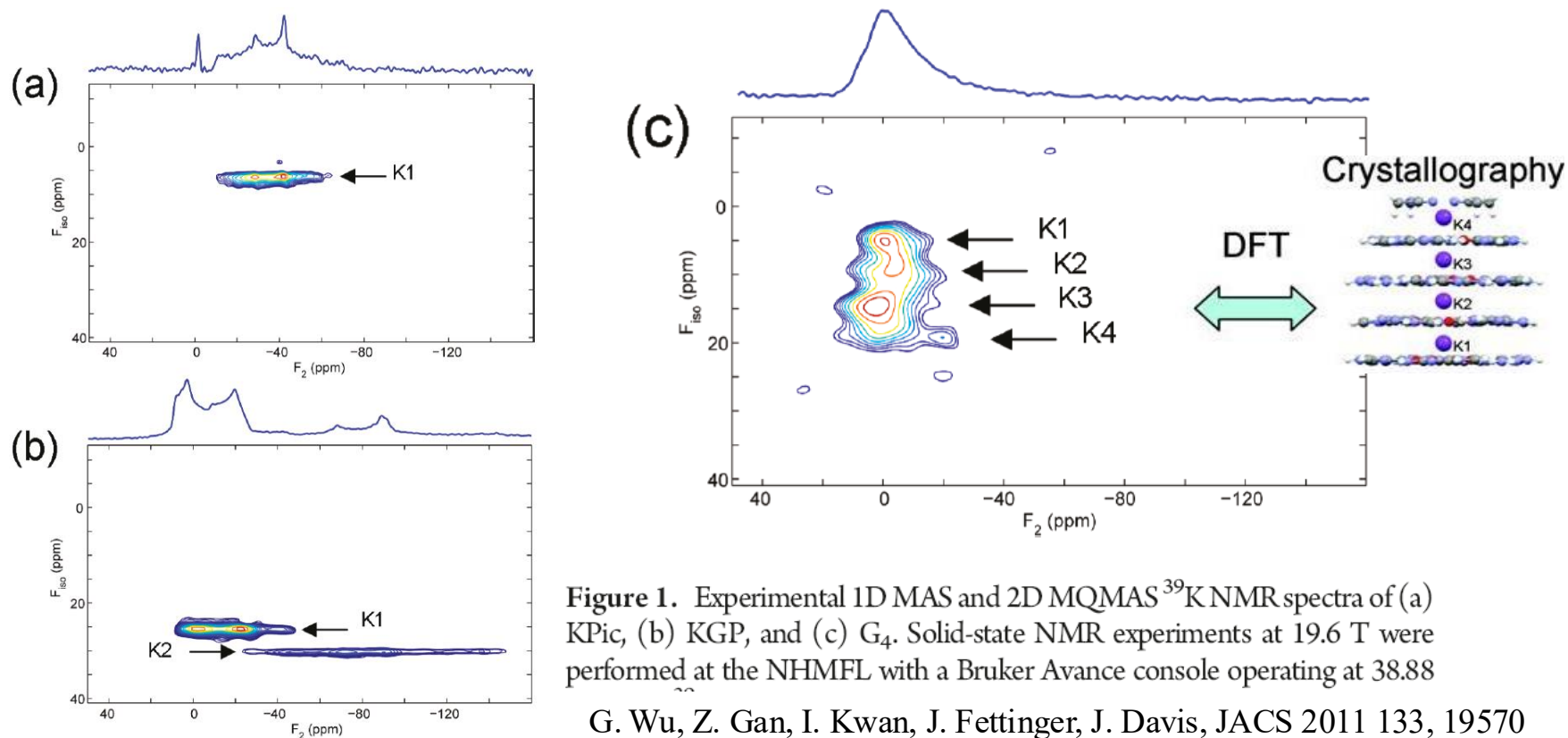


Figure 1. Experimental 1D MAS and 2D MQMAS ^{39}K NMR spectra of (a) KPic, (b) KGP, and (c) G_4 . Solid-state NMR experiments at 19.6 T were performed at the NHMFL with a Bruker Avance console operating at 38.88

G. Wu, Z. Gan, I. Kwan, J. Fetting, J. Davis, JACS 2011 133, 19570



^{25}Mg MQMAS of Layered Double Hydroxide

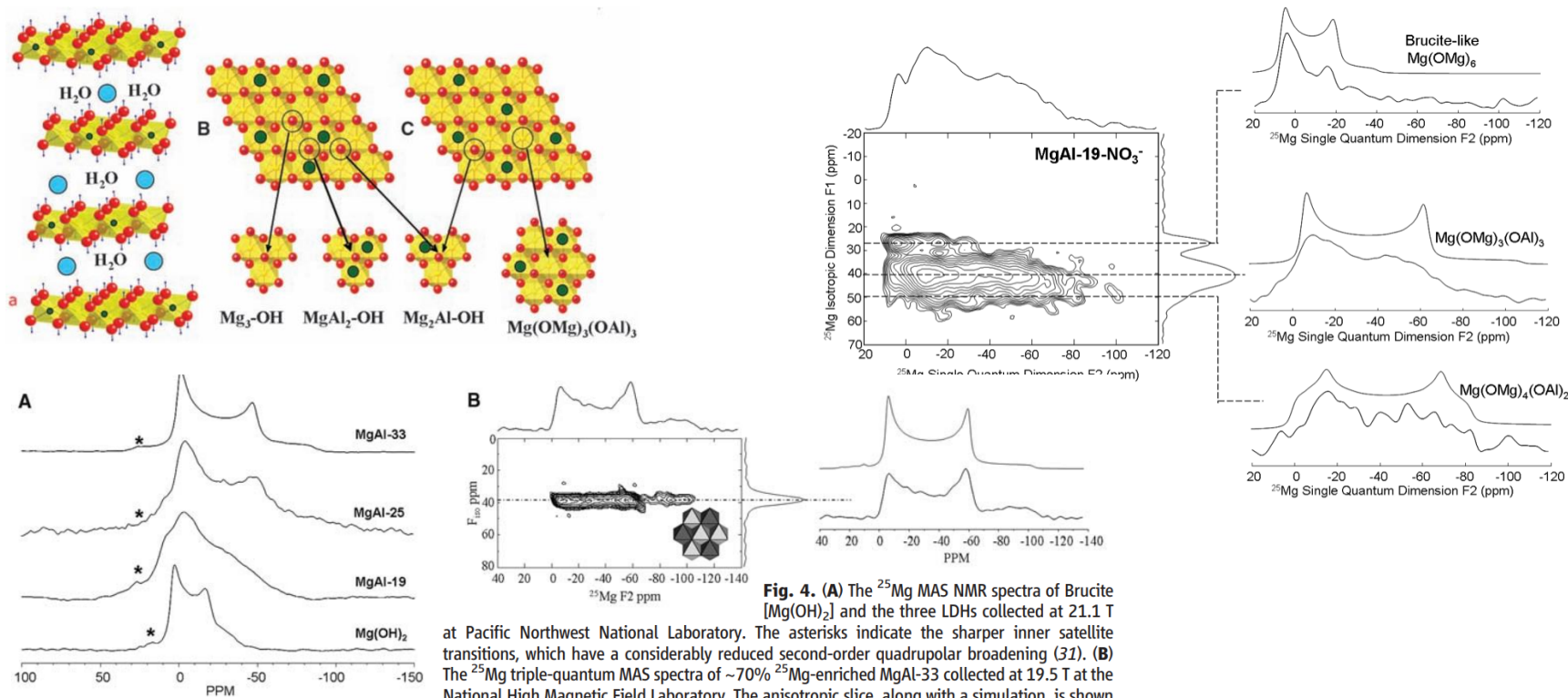


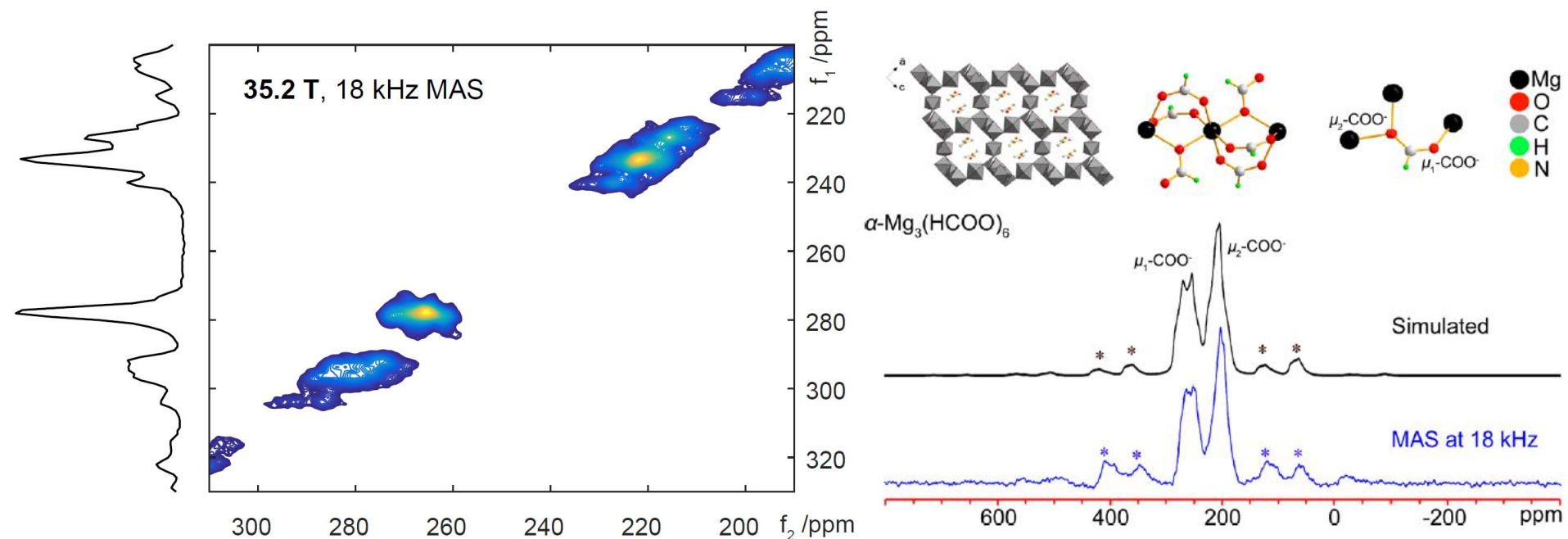
Fig. 4. (A) The ^{25}Mg MAS NMR spectra of Brucite [$\text{Mg}(\text{OH})_2$] and the three LDHs collected at 21.1 T at Pacific Northwest National Laboratory. The asterisks indicate the sharper inner satellite transitions, which have a considerably reduced second-order quadrupolar broadening (31). (B) The ^{25}Mg triple-quantum MAS spectra of $\sim 70\%$ ^{25}Mg -enriched MgAl-33 collected at 19.5 T at the National High Magnetic Field Laboratory. The anisotropic slice, along with a simulation, is shown for the single Mg environment, $\text{Mg}(\text{OAl})_3(\text{OMg})_3$.

P. Sideris, U. Nielsen, Z. Gan, C. Grey *Science*, 321 (2008) 113

<https://doi.org/10.1126/science.aaz0251>



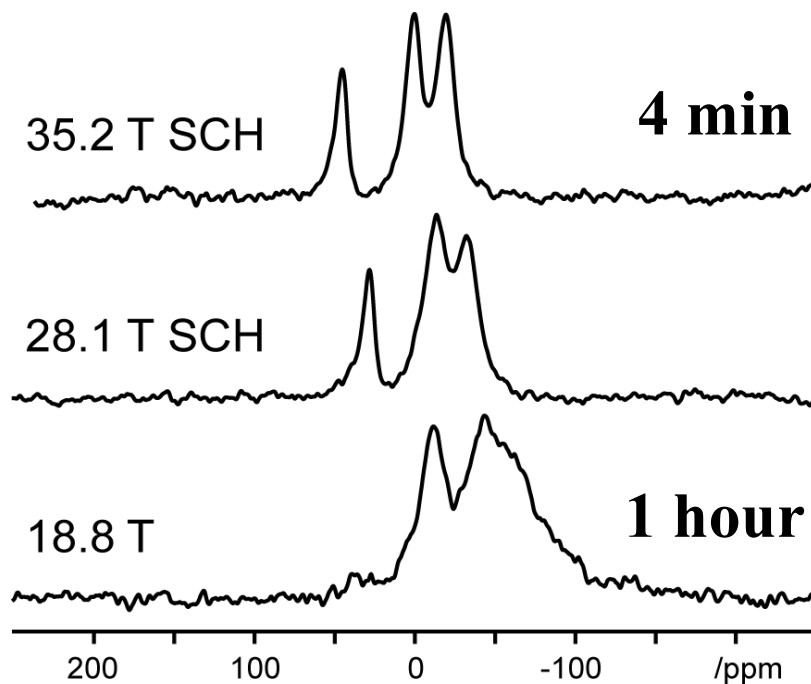
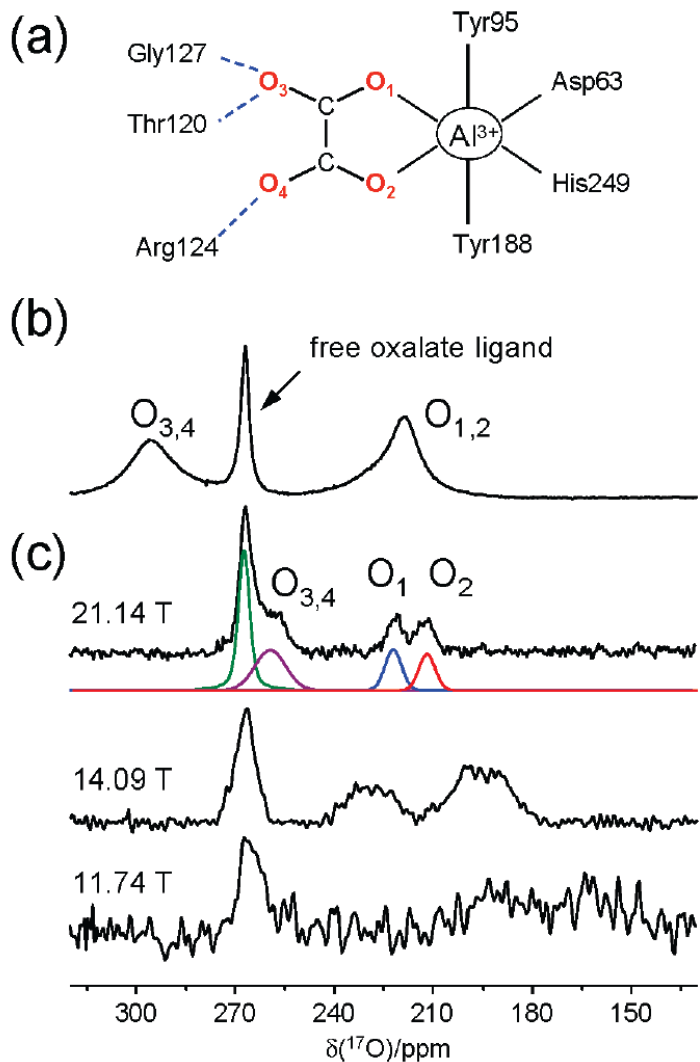
^{17}O NMR of Metal-Organic Frameworks



The high-field and MQMAS reveal more ^{17}O peaks in $\alpha\text{-Mg}_3(\text{HCOO})_6$ MOF that were not observed at 900MHz

Y. Huang U. West Ontario

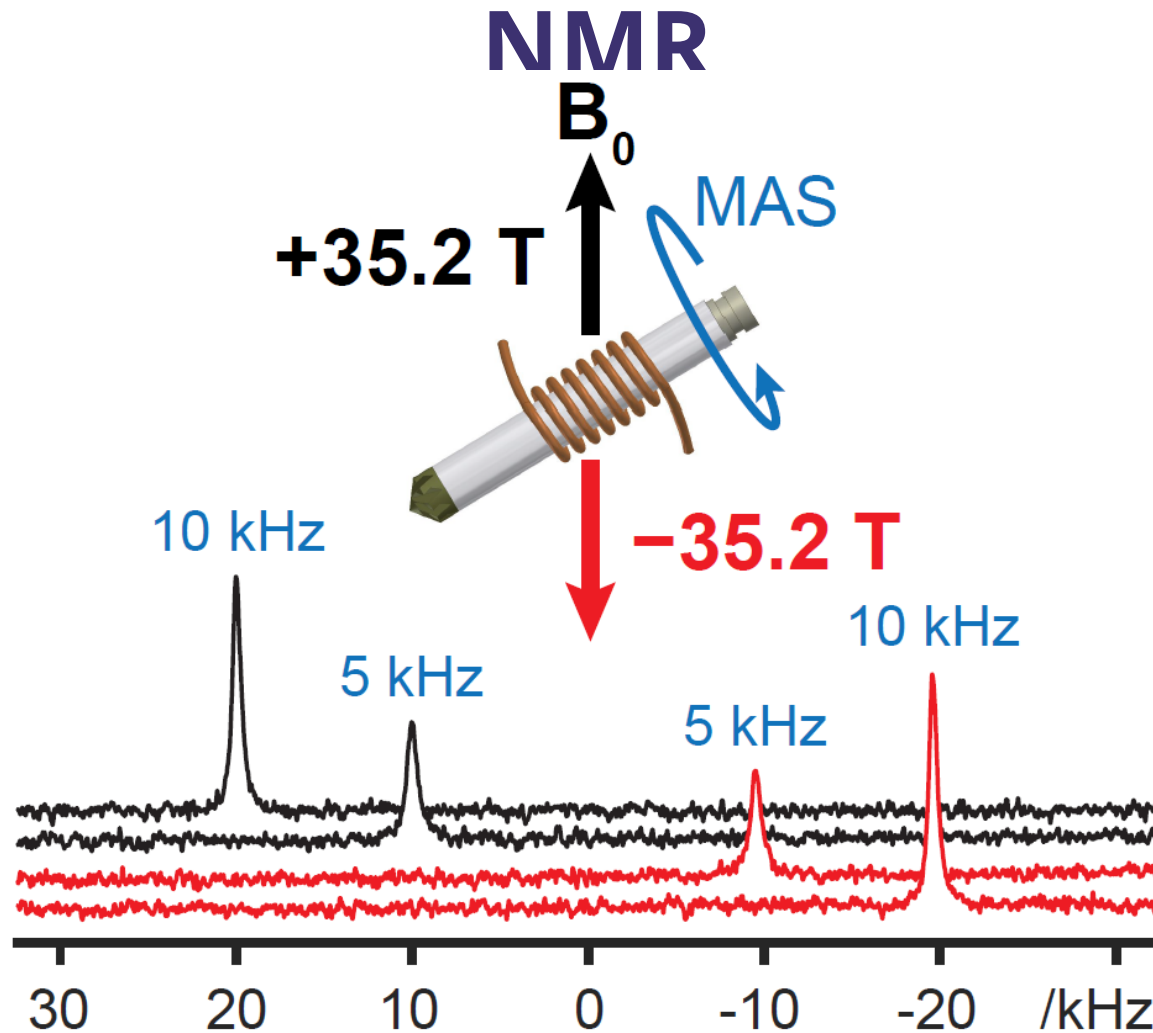
^{17}O QCT Solution NMR



^{17}O quadrupolar central-transition (QCT) spectra of oxalate/chicken ovotransferrin and $[3,5,6-^{17}\text{O}]$ -D-glucose in glycerol.

Gang Wu, Queen's Univ.

Field Reversal of ^{14}N Overtone MAS



^{14}N overtone NMR is direct observation of DQ transition at twice of ^{14}N Larmor frequency. OT peak under MAS shifts at twice of the spinning frequency in a direction depending on the orientation between spinning axis and magnetic field direction.